Original Article

The effects of intermittent hypoxia on hepatic expression of fatty acid translocase CD36 in lean and diet-induced obese mice

Yang Ji [a,1], Yingmin Liang [a,b,1], Pak Hin Chu [b], Mengqin Ge [b], Sze Chun Yeung [b], Mary Sau Man Ip [a,b], Judith Choi Wo Mak [a,b,c,*]

[a] Respiratory Medicine, The University of Hong Kong-Shenzhen Hospital, Shenzhen, China
[b] Department of Medicine, The University of Hong Kong, Hong Kong SAR, China
[c] Department of Pharmacology & Pharmacy, The University of Hong Kong, Hong Kong SAR, China

ABSTRACT

Background: Both obstructive sleep apnea (OSA) and non-alcoholic fatty liver disease (NAFLD) are prevalent within obese individuals. We aimed to investigate the effects of intermittent hypoxia (IH), a clinical feature of OSA, on hepatic expression of fatty acid translocase (CD36) in relation to liver injury in lean and diet-induced obese mice.
Methods: Four-week-old male C57BL/6J mice were randomized to standard diet (SD) or high fat (HF) diet groups. At 13-week-old, all mice were exposed to either air or IH (IH30; thirty hypoxic episodes per hour) for four weeks. We assessed liver injury through lipid profile, oxidative and inflammatory stress, histological scoring and hepatic CD36 expression.
Results: In lean mice, IH elevated serum and hepatic triglyceride and free fatty acid (FFA) levels, in line with upregulation of hepatic CD36 expression and myeloperoxidase (MPO)-positive cells in support of inflammatory infiltrates along with increase in serum malondialdehyde (MDA), C-X-C motif chemokine ligand 1(CXCL-1) and monocyte chemoattractant protein-1 (MCP-1). In diet-induced obese mice, an increase in hepatic alanine transaminase (ALT) activity, serum and hepatic levels of lipid parameters and inflammatory markers, serum MDA level, hepatic expressions of CD36 and α-smooth muscle actin (α-SMA), and MPO-positive cells was observed. IH potentiated hepatic ALT activity, serum CXCL-1 and hepatic interleukin-6 (IL-6), in line with inflammatory infiltrates, but paradoxically, reduced hepatic FFA level and hepatic CD36 expression, compared to obese mice without IH exposure. However, IH further augmented diet-induced liver steatosis and fibrosis as shown by histological scores.
Conclusion: This study contributes to support that IH featuring OSA may lead to liver injury via differential regulation of hepatic CD36 expression in lean and diet-induced obese mice.

* Corresponding author. Departments of Medicine and Pharmacology & Pharmacy, Li Ka Shing Faculty of Medicine, The University of Hong Kong, L8-40 Laboratory Block, 21 Sassoon Rd., Pokfulam, China.
E-mail address: judithmak@hku.hk (J.C.W. Mak).
Peer review under responsibility of Chang Gung University.
[1] These authors contributed equally to the manuscript.

At a glance commentary

Scientific background on the subject

The excess lipid accumulation in the liver, which is not due to alcohol use, is the characteristics of NAFLD. Chronic intermittent hypoxia, a hallmark of OSA, caused triglyceride accumulation in the liver, leading to liver injury and hepatic inflammation.

What this study adds to the field

Our findings shed light on intermittent hypoxia-induced hepatosteatosis without or with obesity via differential regulation of hepatic CD36 expression, which may be relevant to the understanding of the hypothesized role of OSA in the pathogenesis of NAFLD.

Growing prevalence of patients with obstructive sleep apnea (OSA), in which intermittent hypoxia (IH) is a hallmark feature, has become a heavy burden to the healthcare system worldwide [1,2]. Obesity is one of the major risk factors for OSA. Cardiometabolic disorders are common in obese OSA patients, but also in lean patients [3]. Emerging evidence found that OSA and its associated IH is related to non-alcoholic fatty liver disease (NAFLD) [4]. Moreover, data show that OSA independently predicts impaired lipid levels and OSA severity was independently associated with cholesterol and triglyceride concentrations [4]. Therefore, the study between OSA and liver injury resulting in NAFLD progression is attractive. The severity of NAFLD is directly linked to OSA severity and its accompanying IH [5]. However, the mechanism is inconclusive as obesity is a confounder. There is high prevalence of NAFLD in patients with OSA. Independent of obesity and metabolic syndrome, OSA predicts significant hepatic fibrosis in patients with NAFLD [6].

The excess lipid accumulation in the liver, which is not due to alcohol use, is the characteristics of NAFLD. This has now become the most prevalent liver disease worldwide with one-fourth of the population affected, which is in parallel to the epidemic of obesity [7]. Numeral studies have shown that chronic IH caused triglyceride accumulation in the liver, leading to liver injury and hepatic inflammation in mice, which might therefore lead to the progression of NAFLD [5,8]. In addition, many clinical studies have found that OSA is associated with liver injury in obese [9–11] and non-obese patients [12]. Based on animal and human studies, several pathophysiological mechanisms have emerged to explain the link between OSA/IH and liver injury, in which lipid dysfunction may play an important role.

Liver, a central regulator of lipid homeostasis, is accountable for the regulation of new fatty acid synthesis, their export and subsequent redistribution to other tissues, as well as their usage as energy substrates [13]. The uptake of circulating fatty acids by the liver is mainly relied on fatty acid transporters including cluster of differentiation 36 (CD36), also known as fatty acid translocase [14]. It is known that CD36 plays a role in lipid metabolism via facilitating intracellular free fatty acid (FFA) uptake and trafficking, as well as esterification of FFAs into triglycerides in cardiac and skeletal muscle cells [15]. Upregulation of CD36 expression was in parallel to hepatic triglyceride content in different animal models of obesity with liver injury [16,17]. One recent report found elevation of intrahepatic expression of CD36 in OSA patients as well as in IH-exposed mouse model [18]. However, there is currently a lack of study on the role of CD36 linking OSA, obesity and liver injury. Therefore, we aimed to determine the effects of IH on hepatic CD36 expression, in relation to lipid profiles and oxidative and inflammatory markers, and liver injury using an IH-exposed mouse model in lean and diet-induced obese mice.

Materials and methods

Experimental animals

Four-week-old male C57BL/6J mice were purchased from the Laboratory Animal Unit at the University of Hong Kong. All mice were housed in a well-regulated pathogen-free environment (temperature: 22 ± 1 °C; humidity: 65–70%) on a 12/12-h light/dark cycle with free access to food and water. Animal care and experimental protocol for the study were approved by the Committee on the Use of Live Animals in Teaching and Research (CULATR, No. 3795–15) at the University of Hong Kong. All animal experiments complied with the ARRIVE guidelines and were performed in compliance with the UK Animals (Scientific Procedures) Act, 1986 and associated guidelines, and the EU Directive 2010/63/EU.

Experimental design and animal model of intermittent hypoxia (IH)

The mice were randomly fed with low fat laboratory standard diet (SD) [composed of 20% protein, 5% fat, 4.7% fiber and 52.9% carbohydrate; 3.41 kcal/g; LabDiet, 5053 (LabDiet; St. Louis, MO, USA)] or high fat (HF) diet [composed of 24% protein, 24% fat, 5.8% fiber and 41% carbohydrate; 4.73 kcal/g; D12451 (Research Diet, New Brunswick, NJ, USA)] respectively. The consumption of diets and the gain of body weight were examined every week. At the age of 13-week, the mice were further divided into two subgroups and exposed to either air (2 groups) or intermittent hypoxia (IH; 2 groups) for four weeks (n = 6 for each group). The IH protocol had been described in our previous study [19]. During the air/IH exposure, the mice were continued their SD or HF diet respectively. Total fat mass and total lean mass were assessed by the Minispec LF90 Body Composition Analyzer (Bruker, Billerica, MA, USA) before sacrifice. Mice were sacrificed with overdose of sodium pentobarbital anesthesia (100 mg/kg, i.p.) after fasting overnight. Serum samples and liver tissues were collected, frozen in liquid nitrogen before keeping in −80 °C freezer for further use.

Protein extraction

A small piece of liver tissues from each mouse was ground up to powder with mortar and pestle in liquid nitrogen before homogenization in T-PER tissue protein extraction reagent (Cat. # 78510; ThermoFisher Scientific, Rockford, IL, USA) containing protease/phosphatase inhibitors cocktail (1:100; Cat. # 78440; ThermoFisher Scientific) and 100 mM phenyl-methanesulfonyl fluoride (PMSF) before sonication. The suspensions were centrifuged at $14,000 \times g$ for 15 min at 4 °C and the supernatants were collected as total protein. The protein concentration was measured by Bradford protein assay (Bio-Rad Laboratories, Hercules, California, USA).

Lipid extraction and measurement

Lipid extraction from the frozen liver tissue was carried out according to the established protocol [20]. Briefly, liver tissues (~20 mg) were weighted before placing in lipid extraction buffer (2 volume chloroform and 1 volume methanol). After vigorously vortex, the tissue was incubated for 16 h at 4 °C. Sodium chloride (0.6%, 2 ml) was added and the mixture was centrifuged at $2000 \times g$ for 20 min to separate the organic (bottom) layer of the liquid for collection before evaporation of the organic solvent using Savant™SC110A Speed Vac Plus concentrator with Universal Vacuum System Plus (Thermo Scientific). Lipid dissolution buffer (5 volume isopropanol, 2 volume water and 2 volumes of Triton X-100) was applied to the pellet before measurements of lipid parameters.

Levels of serum and hepatic cholesterol and triglyceride were determined with commercial kits from Stanbio Laboratory (Cat #1010 and 2100; Boerne, TX, USA) according to manufacturer's instructions. Serum and hepatic FFA levels were measured by half-micro test kit from Roche (Cat # 11-383-175-001, Roche Applied Science, Mannheim, Germany). Levels of hepatic lipid parameters were corrected by the protein concentration of the aqueous (top) layer during the extraction.

Biochemical assay

Levels of alanine aminotransferase (ALT), and malondialdehyde (MDA) in serum or/and liver were determined using commercial kits from Nanjing Jiancheng Bioengineering Institute (Nanjing, China) according to the manufacturer's instructions.

Enzyme-linked immunosorbent assay (ELISA)

Levels of C-X-C motif chemokine ligand 1 (CXCL-1) and monocyte chemoattractant protein-1 (MCP-1) in serum and liver tissue, and the levels of interleukin-6 (IL-6) and tumor necrosis factor α (TNF-α) in liver tissue were measured by commercial enzyme-linked immunosorbent assay (ELISA) kits from R&D System (Cat # DY453, DY479Minneapolis, USA) or Thermo Scientific (Cat # 88-7064, 88-7324 Rockford, IL, USA) respectively. The Absorbance was measured at wavelength 450/570 nm in a microplate reader (CLARIOstar®, BMG Labtech, Ortenberg, Germany). Levels of each parameter in liver tissue were corrected with the protein concentration of each sample.

Western blot analysis

Protein samples (60 μg) were separated by sodium dodecyl sulfate polyacrylamide gel electrophoresis (SDS-PAGE) method, which is transferred onto the nitrocellulose membrane. After blocking in 5% non-fat milk, the membranes were incubated with diluted specific primary antibodies fatty acid translocase (FAT)/CD36 (CD36 at 1:500, Cat# NB110-59724, Novus Biologicals, Littleton, CO, USA) and α-smooth muscle actin (α-SMA at 1:2000, YM3364, ImmunoWay Biotechnology Company, Plano, TX, USA) overnight at 4 °C. The membranes were then probed with horseradish peroxidase (HRP)-conjugated goat-anti-rabbit or HRP-conjugated goat-anti-mouse IgG secondary antibodies (Cat#NB7160, NB7544, Novus Biologicals, Littleton, CO, USA, 1:5000), and visualized by the ChemiDoc MP Imaging System (Bio-Rad Laboratories, Inc.) using enhanced chemiluminescence (ECL; RPN2106, Amersham Biosciences, GE Healthcare, Chicago, Illinois, USA). Densitometry analysis of the bands was performed on the scanned films using GelQuant.NET version 1.8.2, normalized against the loading control (β-actin), and graphically expressed as fold change relative to control condition.

Immunohistochemistry

Formalin-fixed, paraffin-embedded liver blocks were cut into 5-μm-thick tissue sections, deparaffinized, and rehydrated. The sections were firstly steamed in 0.01M sodium citrate buffer (pH 6.0) at 120 °C for 20 min to perform antigen retrieval, treated with 3% H_2O_2 for 15 min to inhibit endogenous peroxidase, and then blocked with 2.5% goat serum. Afterward, the sections were incubated in a humidified chamber with the first antibodies directed against myeloperoxidase (MPO, Cat# ab9535 Abcam, San Francisco, CA, USA) at 1:100, hypoxia-inducible factor-1 alpha (HIF-1α, Cat# NB100-105, Novus, Biologicals, Littleton, CO, USA) at 1:100 or CD36 at 1:100 overnight at 4 °C. Negative controls were carried out by incubating with isotype-specific rabbit IgGs instead of the specific primary antibody. After washing, the slides were covered with biotinylated secondary antibody. Slides were washed and developed with DAB substrate (Cat #K3468, Dako, Santa Clara, CA, USA). Slides were dehydrated and mounted with coverslips.

Histological examination

Hematoxylin and eosin (H&E) staining, and Sirius Red staining were carried out for histologic examination on formalin-fixed paraffin-embedded 5 μm liver sections using H&E solutions from Sigma—Aldrich (St. Louis, MO, USA), and Picro Sirius Red Stain kit from Abcam (#ab150681, San Francisco, CA, USA) respectively. Images were captured using Nikon microscope (Nikon Instruments Inc., Tokyo, Japan) with a Nikon DS-Ri2 Digital Camera. The modified histological scoring was determined by the presence of steatosis, hepatic inflammation and fibrosis according to the previous publication [21].

Statistical analysis

All data were presented as mean $\pm$ standard error of mean (SEM) for indicated number of animals (n). One-way analysis
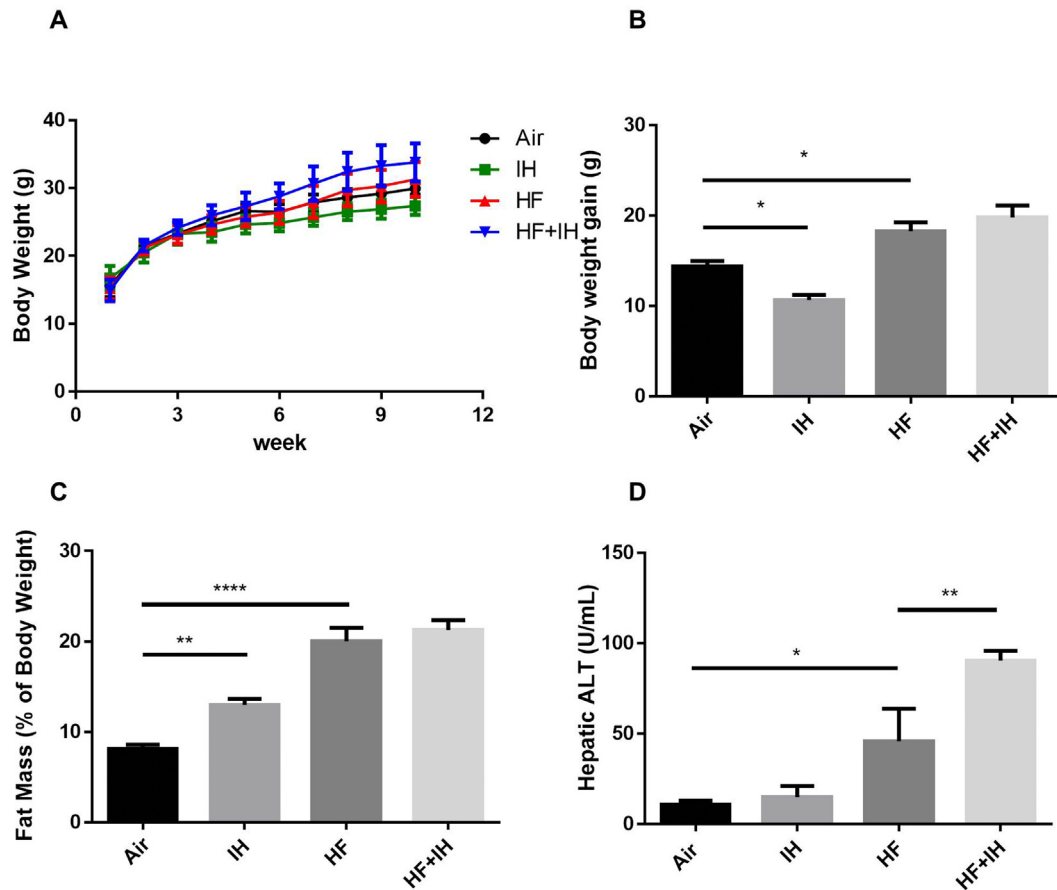
Fig. 1 Body weight, fat mass and hepatic marker of liver injury. (A) Body weight of each mouse during the entire experimental period. (B) Body weight gain of each mouse at the end of the experiment. (C) Fat mass (%) of body weight at the end of the experiment. (D) Hepatic alanine aminotransferase (ALT) activity. Data are expressed in mean $\pm$ standard error of mean (SEM) (n = 6 each group). $*p < 0.05$, $**p < 0.01$, $****p < 0.0001$ for one-way ANOVA test with *post hoc* analysis (Bonferroni) among different groups.

of variance (ANOVA) followed by the *post hoc* Bonferroni's test was performed for comparison among multiple groups. The comparison between two different groups was carried out by unpaired student's *t* tests where appropriate. All the statistical analyses were conducted using GraphPad Prism 7.0 (GraphPad Software Inc., San Diego, CA, USA). Differences were considered statistically significant at *p* value of < 0.05.

Results

Metabolic characteristics of experimental groups

Despite significant elevation of IH-induced fat mass and food consumption in lean mice, there was a significant reduction of body weight gain but no effect on hepatic ALT activity after IH compared to air-exposed group. Although there was a reduction in food consumption throughout the study period, HF diet alone caused significant increase in body weight gain, fat mass and hepatic ALT activity compared to lean mice (Supplementary Fig. 1A). In diet-induced obese mice, IH caused no further effects on body weight gain and fat mass

but further potentiation of hepatic ALT activity, indicating severe liver injury [Fig. 1A–D].

In lean mice, IH caused upregulation of serum and hepatic levels of triglyceride and FFA but reduction in serum cholesterol level compared to air-exposed group. HF diet alone led to increased levels of serum and hepatic cholesterol, triglyceride and FFA in comparison to lean mice. In diet-induced mice, IH caused only reduction in hepatic FFA but no other lipid parameters in serum and liver [Fig. 2A–F].

Presence of oxidative stress in serum and liver

IH caused significant elevation in serum level of MDA in lean mice compared to air-exposed group. HF diet alone also led to upregulation of serum MDA level but no further effect after IH in HF diet-induced obese mice [Fig. 3A]. From immunohistochemical staining, it was possible to detect only a few cells by MPO on liver sections. The MPO-positive cells were scattered, mostly round and had little cytoplasm. IH was associated with a diffuse increase in the number of MPO-positive cells in liver parenchyma of lean mice, indicating neutrophil infiltration and activation that might result in the release of granules
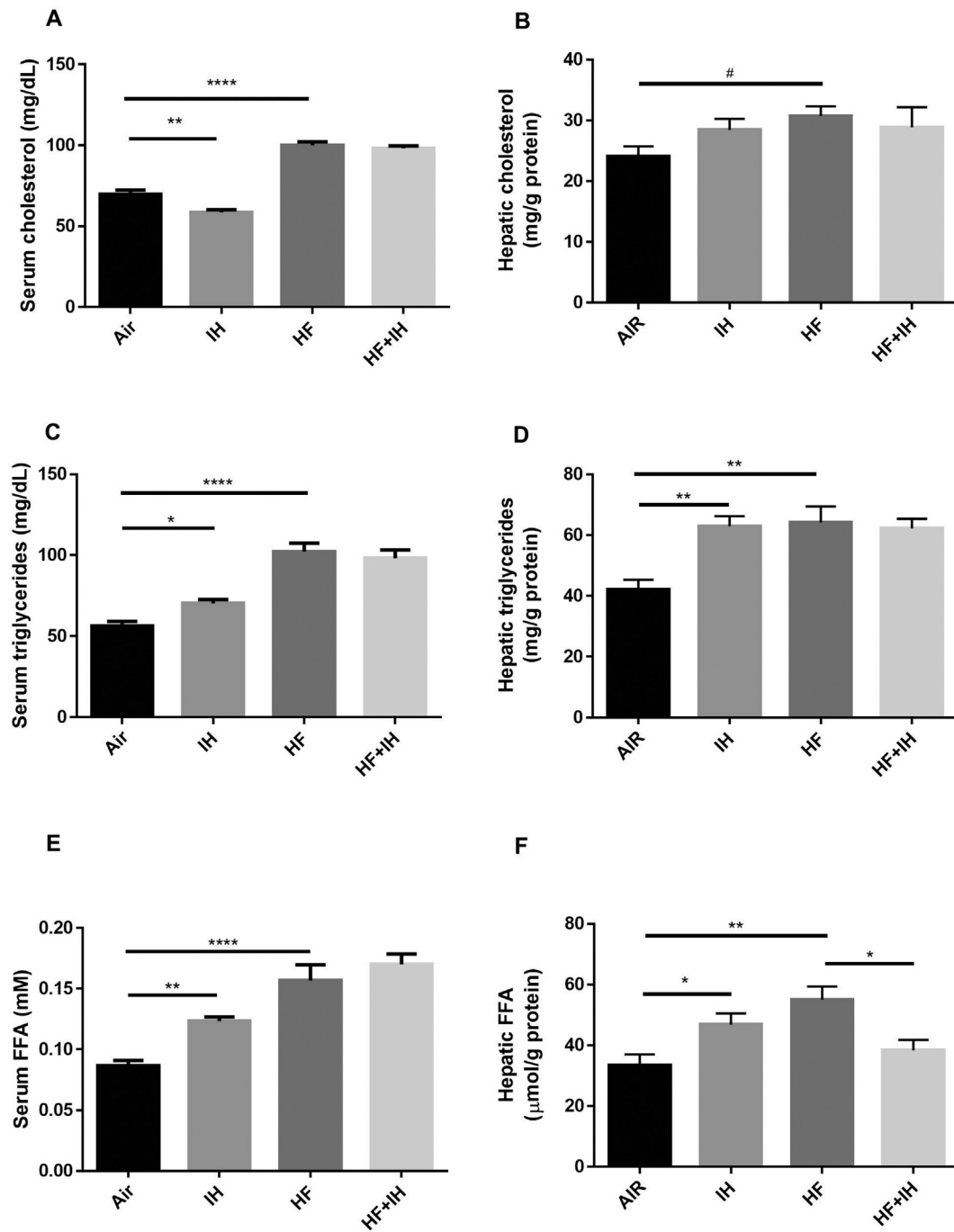
Fig. 2 Serum and hepatic lipid levels. Cholesterol levels in serum (A) and liver (B), triglyceride levels in serum (C) and liver (D), and free fatty acid (FFA) levels serum (E) and liver (F), were measured by commercial biochemistry assay kits. Data are expressed in mean ± standard error of mean (SEM) (n = 6 each group). *$p < 0.05$, **$p < 0.01$, ****$p < 0.0001$ for one-way A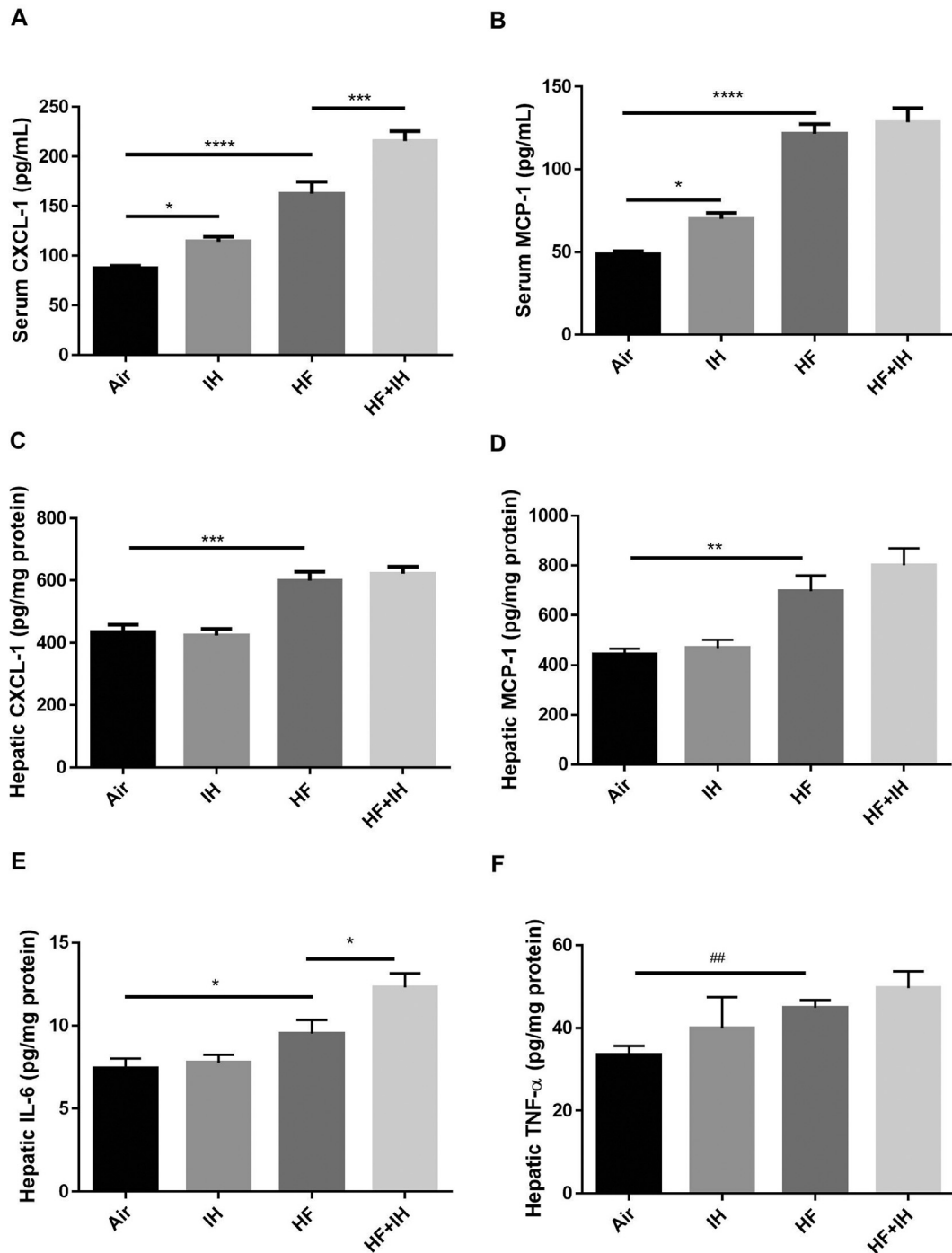NOVA test with *post hoc* analysis (Bonferroni) among different groups; [#]$p < 0.05$, for unpaired student's *t* test between two groups.

containing reactive oxygen species (ROS) to enhance the acute inflammatory response. HF diet also led to elevation of MPO-positive cells with further elevation after IH in liver parenchyma of diet-induced obese mice [Fig. 3B]. Furthermore, immunohistochemical staining revealed that the positive expression of HIF-1α was remarkably upregulated in the nuclei of hepatocytes after IH in lean mice [Fig. 3C]. HF diet alone caused only a slight increase in HIF-1α-positive cells

with further upregulation after IH in the nuclei of hepatocytes compared to the SD control [Fig. 3C].

Presence of inflammation in serum and liver

In lean mice, IH led to elevation of serum but not hepatic levels of CXCL-1 and MCP-1 in comparison to air-exposed group. HF diet alone caused significant upregulation of
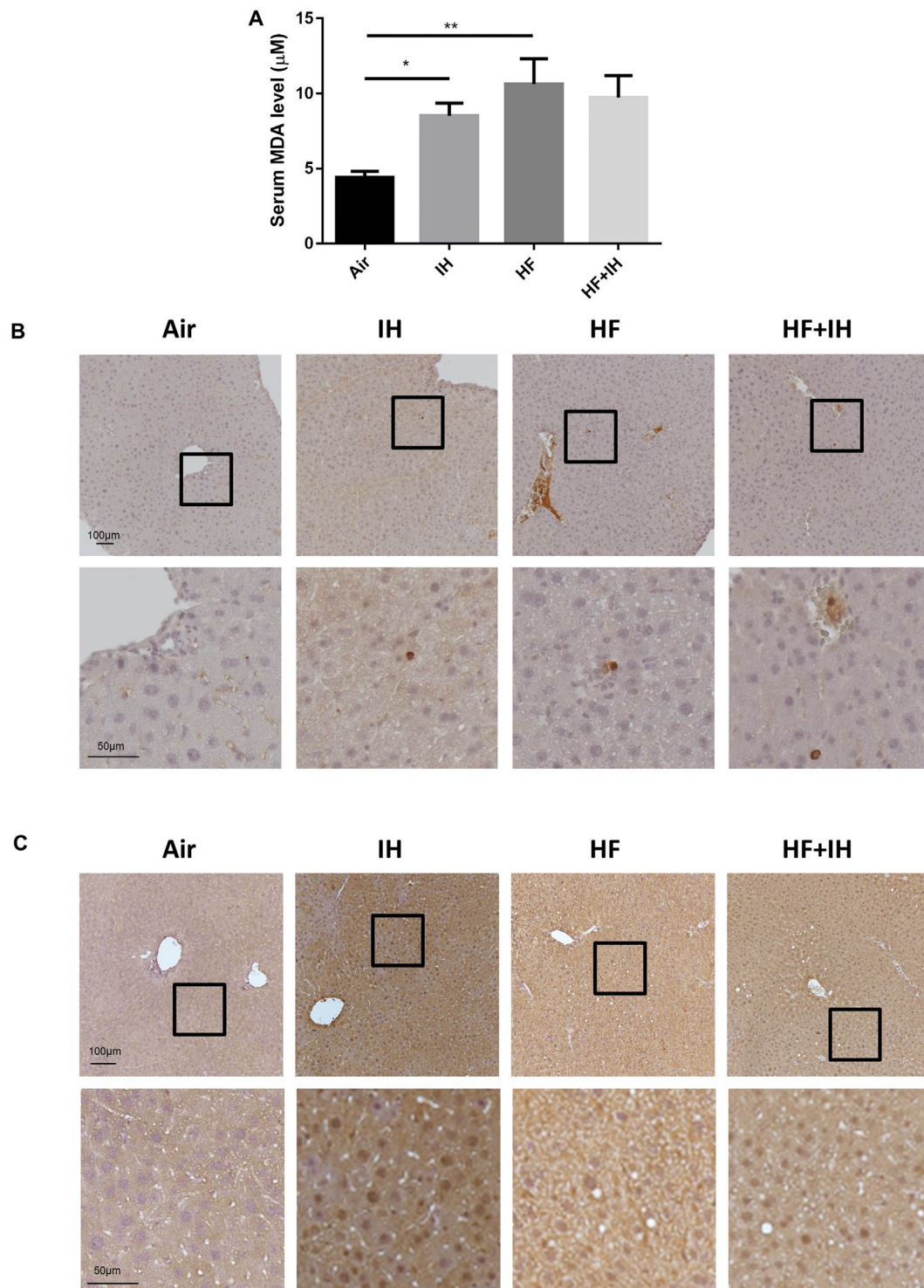
Fig. 3 Presence of oxidative stress in serum and liver. (A) Serum malondialdehyde (MDA) level. (B) Representative images of immunohistochemical detection of myeloperoxidase (MPO) on the liver sections. Upper panel in B shows MPO-positive cells in hepatocytes, scale bar = 100 μm; lower panel in B shows higher magnification of the selected area from the upper panel, scale bar = 50 μm. (C) Representative images of immunohistochemical detection of hypoxia-inducible factor-1 alpha (HIF-1α) on the liver sections. Upper panel in B shows HIF-1α-positive staining in the nuclei of hepatocytes, scale bar = 100 μm; lower panel in B shows higher magnification of the selected area from the upper panel, scale bar = 50 μm. Data are expressed in mean ± standard error of mean (SEM) (n = 6 each group). *$p < 0.05$, **$p < 0.01$ for one-way ANOVA test with *post hoc* analysis (Bonferroni) among different groups.

Fig. 4 Presence of inflammation in serum and liver. Levels of C-X-C motif chemokine ligand 1 (CXCL-1) in serum (A) and liver (B), levels of monocyte chemoattractant protein-1 (MCP-1) in serum (C) and liver (D), level of interleukin-6 (IL-6) (E) and tumor necrosis factor α (TNF-α) (F) in the liver were detected by commercial ELISA kits. Data are expressed in mean $\pm$ standard error of mean (SEM) (n = 6 each group). *$p < 0.05$, **$p < 0.01$, ***$p < 0.001$, ****$p < 0.0001$ for one-way ANOVA test with *post hoc* analysis (Bonferroni) among different groups; ##$p < 0.01$ for student's *t* test between two groups.

serum and hepatic levels of CXCL-1 and MCP-1 as well as hepatic levels of IL-6 and TNF-α compared to lean mice. In diet-induced obese mice, IH also led to potentiation of serum level of CXCL-1 and hepatic level of IL-6 [Fig. 4A–F]. However, serum levels of IL-6 and TNF-α were below the detectable limit of the commercially available kits in this study.

Hepatic cluster of differentiation 36, also known as fatty acid translocase (CD36) expression

IH caused upregulation of hepatic CD36 expression in lean mice compared to air-exposed group. HF diet alone led to significant increase in hepatic expressions of CD36 and α-SMA. In diet-induced obese mice, IH caused significant
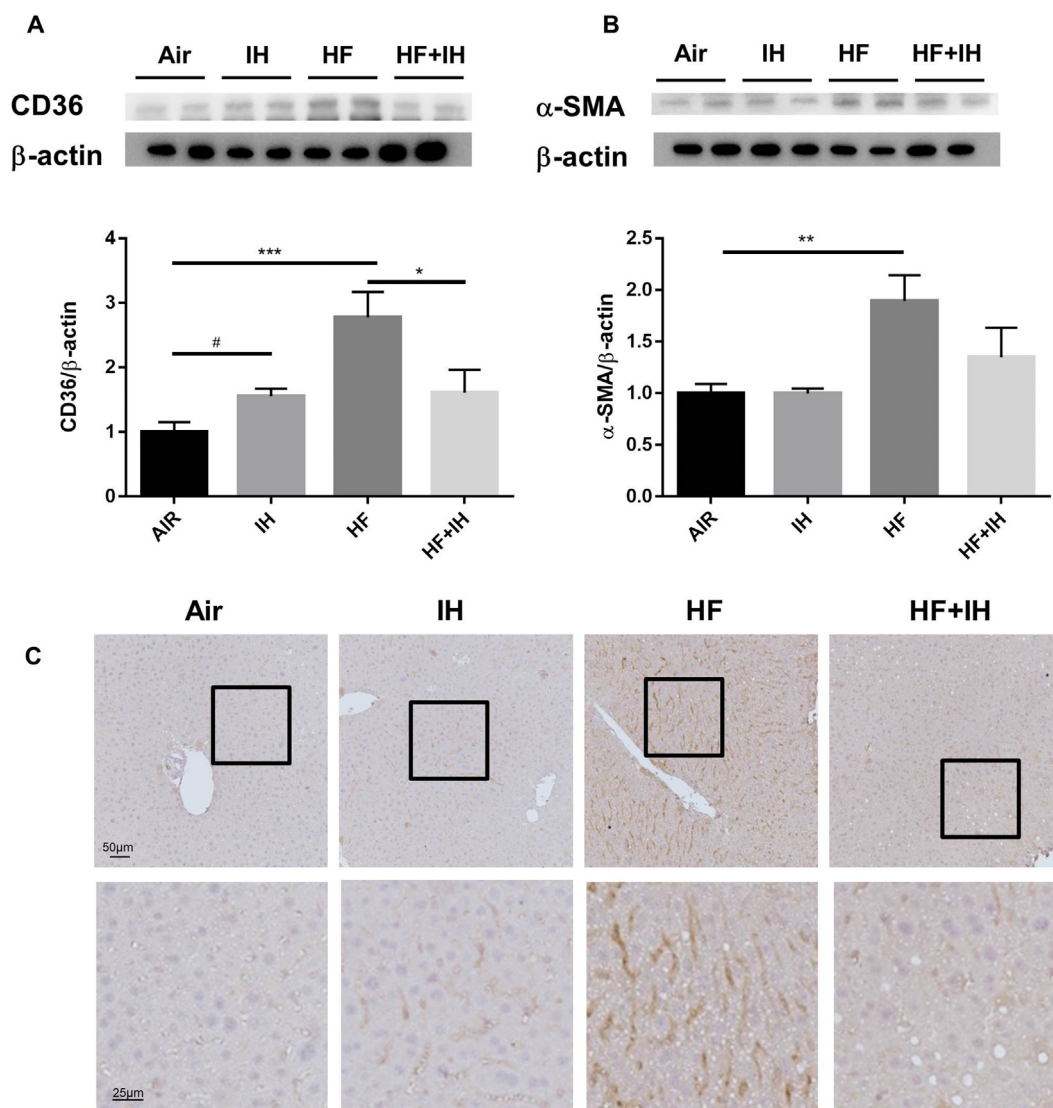
Fig. 5 Protein expressions of CD36 and α-smooth muscle actin (α-SMA) as well as localization of CD36 in the liver. Protein expressions of CD36 (A) and α-SMA (B) were detected by Western blot analysis. (C) Representative images of immunohistochemical detection of CD36 on the liver sections. CD36-positive cells were present in the hepatocytes; upper panel: scale bar = 50 μm; lower panel: scale bar = 25 μm *$p < 0.05$, **$p < 0.01$, ***$p < 0.001$, for one-way ANOVA test with *post hoc* analysis (Bonferroni) among different groups; #$p < 0.05$ for student's *t* test between two groups.

reversal of HF diet-induced upregulation of hepatic CD36 expression and a trend of reduction in hepatic α-SMA expression [Fig. 5A and B].

In parallel, the signal from immunohistochemical staining of CD36 was found in plasma membrane and cytoplasm of hepatocytes of mouse livers with the highest intensity of signal in diet-induced obese mice and a reduction after IH exposure [Fig. 5C].

Histological assessment in liver

Histological assessment of the liver with the established scoring system showed no hepatic steatosis in lean mice without IH but only occasionally retrievable in lean mice with IH. The presence of hepatic macrovesicular and micro-vesicular steatosis was found in diet-induced obese mice

without or with IH [Fig. 6A and C]. IH alone led to the presence of inflammatory infiltrates, which was evidenced by H&E staining in lean mice compared to air-exposed lean mice, which was further augmented in diet-induced obese mice [Fig. 6A and C]. Upregulation of collagen fibers was seen in IH-exposed lean mice and HF diet-induced obese mice, as illustrated by Sirius Red staining, which was further enhanced by IH in the diet-induced obese mice, indicating the presence of liver fibrosis [Fig. 6B and C]. In general, our model mainly displayed early onset of disease stages.

Discussion

This study observed the differential influence of IH or/and HF diet on lipid profile, oxidative and inflammatory status and
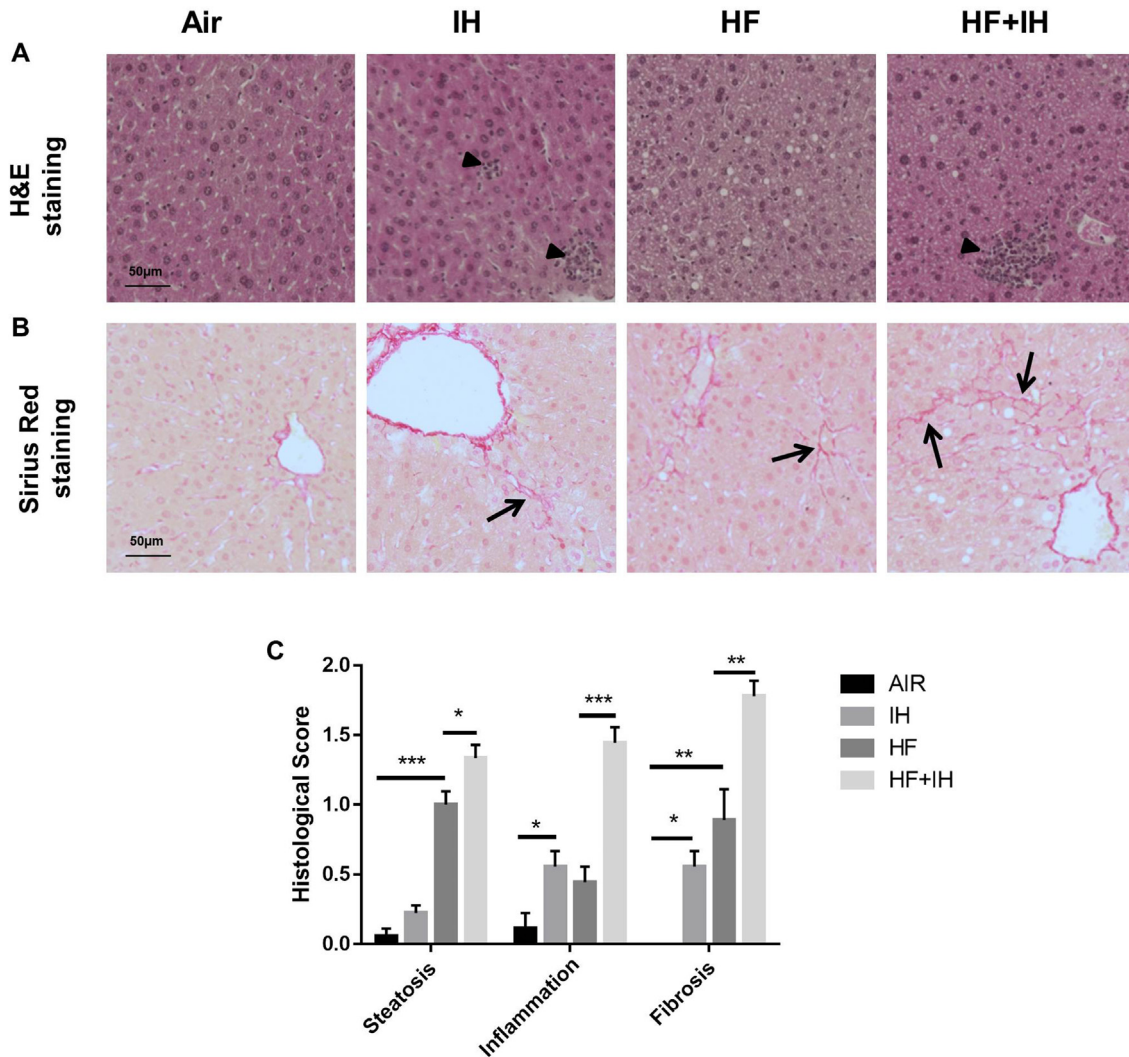
Fig. 6 Histological assessment on liver sections. (A) Representative images of Hematoxylin & Eosin (H&E) staining. Black arrow heads indicate the inflammatory infiltrates on liver sections. (B) Representative images of Sirius Red staining. Black arrows indicate collagen fibers on liver sections. Scale bar = 50 μm. (C) Histological scoring was determined by the presence of steatosis, inflammation and fibrosis on liver sections as previously described with slight modification [21]. *$p < 0.05$, **$p < 0.01$, ***$p < 0.001$, for one-way ANOVA test with *post hoc* analysis (Bonferroni) among different groups.

hepatic expression of CD36 in relation to histological examination. The findings showed that IH exposure in lean mice reduced body weight gain with a reduction in serum cholesterol level but an increase in fat mass, and despite no elevation of hepatic ALT activity, levels of serum and hepatic triglyceride and FFA were increased, in line with upregulation of hepatic CD36 expression and the presence of inflammatory infiltrates and collagen deposition on liver sections, indicating liver injury. In diet-induced obese mice, IH exposure caused potentiation of obesity-induced hepatic ALT activity, inflammatory infiltrates, collagen deposition, serum CXCL-1 and hepatic IL-6, but inhibition of hepatic level of obesity-induced FFA and hepatic CD36 expression.

Many reports on patients with different OSA severity have demonstrated that IH may play an independent role in the development and progression of NAFLD [4,10,22]. Repeated IH is associated with systemic oxidative and inflammatory stress in peripheral tissues in rodent models [23–25], in agreement with this study. In addition, IH has been found to increase hepatic steatosis and fibrosis in lean and obese rodent models [26–28]. Our finding of IH-induced reduction in serum cholesterol level in lean mice was contradictory to previous reports, which found elevation of serum cholesterol levels after different durations of IH with either no difference (5-day IH) or reduction (12-week IH) in hepatic cholesterol levels [26,29]. In contrast, another study found that IH (6-month) increased hepatic cholesterol content without effect on serum cholesterol level in high fat high cholesterol (HFHC) diet-induced obese mice [27]. In our study, hepatic cholesterol levels were not affected by IH in the HF diet-induced obese mice. This discrepancy of results is not surprising as HF diet and HFHC diet may affect lipid metabolism differentially through gut microbiota in mice [30]. As the liver produces and clears cholesterol in the body, the decrease in serum cholesterol of IH-induced lean mice may be due to increased clearance of cholesterol. On the other hand, triglyceride and FFA

levels were elevated in liver tissue of IH-exposed lean mice, in parallel to an increase in serum triglyceride and FFA levels. However, IH did not cause further enhancement of HF diet-induced upregulation of serum cholesterol, triglyceride and FFA levels. Nevertheless, HF diet-induced increase in hepatic cholesterol and triglyceride levels remained unchanged but a reduction of HF-induced elevation of hepatic FFA was observed. These findings indicate differential role of IH on fatty acids in the liver of lean and diet-induced obese mice via alterations in fatty acid β-oxidation (FAO), very low density lipoprotein (VLDL) secretion, and pathways involved in the synthesis of fatty acids [31]. The increase in hepatic FFA may result in an increase in the synthesis of triglycerides in the liver, in agreement with our findings. The increase in serum triglycerides may be due to increased hepatic production of VLDL particles and a decrease in the clearance of triglyceride rich lipoproteins. The rate of secretion of VLDL particles is highly dependent on triglyceride availability, which is determined by the levels of FFA available for the synthesis of triglycerides in the liver. In addition, our results showed that IH caused significant increase in fat mass despite a reduction in body weight gain in lean mice, which may lead to the accumulation of fat within the body, in line with the upregulation of serum and hepatic triglyceride and FFA levels.

Previous publications have demonstrated that IH of OSA is indistinguishable to ischemia/reperfusion injury in which it can generate large amount of ROS, resulting in oxidative stress [32]. In order to show that IH can raise liver oxidative stress, we measured serum level of MDA and examined MPO immunohistochemical staining on liver sections. MDA, acting as a lipid peroxidation marker, is one of the final products of polyunsaturated fatty acid peroxidation in cells. MPO, acting as an oxidative stress marker, is an important peroxidase released in the azurophilic granule of activated neutrophils [33]. MPO has been shown to be expressed only by neutrophils in normal and in inflamed liver [34]. In this study, elevation of serum levels of MDA was observed in IH-exposed lean mice and in diet-induced obese mice, but IH caused no further increase in serum MDA level in diet-induced obese mice. On the other hand, IH caused an increase in the number of MPO-positive cells in lean mice, in support of enhanced oxidative stress. Immunohistochemical study of the liver sections found that IH exposure led to more MPO-positive cells present on liver sections of diet-induced obese mice, suggesting an increase of neutrophil infiltration, which is an important feature promoting development of liver injury [27,35]. Neutrophil infiltration is linked to liver inflammation and subsequent inflammation-induced liver injury [36,37].

IH is known to stimulate the production of ROS, which in turn may activate the pro-inflammatory transcription factor nuclear factor kappa-light-chain-enhancer of activated B cells (NF-κB) pathway [38], resulting in elevated expressions of its downstream targeted genes such as IL-6, IL-8 and TNF-α. In line with previous reports [39,40], we showed that IH caused elevation of serum levels of CXCL-1 and MCP-1 in lean mice, and potentiation of diet-induced upregulation of serum level of CXCL-1 but not serum MCP-1 in diet-induced obese mice. IH also led to potentiation of hepatic level of IL-6 but not TNF-α in diet-induced obese mice, in agreement with previous finding [27]. CXCL-1 has neutrophil chemotactic activity and increases

neutrophil infiltration in the liver [41]. Moreover, an increase in MPO-positive cells after IH in the liver of lean and diet-induced obese mice suggests that neutrophil activation in liver tissue could be another source of oxidative stress in IH-induced liver injury. Elevation of hepatic IL-6 by IH in diet-induced obese mice may have a detrimental effect on the liver, in line with the findings of IL-6-activated apoptosis and inflammation in liver [42].

Studies have shown that CD36 not only acts as one of the FFA transporters, but also regulates FAO, lipid synthesis, VLDL secretion, inflammation and autophagy in liver cells [43]. Nevertheless, there was a reduction in oxidation of exogenous FFAs in *Cd36*-deficient mice or human with impaired FFA uptake [44]. One previous report also found enhanced FAO of endogenous triglyceride stores in myocytes of *Cd36*-knockout mice by an AMPK-dependent mechanism, linking FFA uptake to FAO via CD36 [45]. Under normal conditions, the expression of CD36 in the hepatocytes is rather weak, but its expression in the liver is highly inducible by lipid overload. In line with previous reports [16–18], we found that hepatic CD36 expression increased concomitantly with hepatic triglyceride level, the best measure of steatosis, in IH-exposed lean mice and diet-induced obese mice in this study. Despite IH-induced potentiation of systemic CXCL-1 level and hepatic IL-6 level in diet-induced obese mice, IH attenuated the HF diet-induced upregulation of hepatic CD36 concomitant with a reduction of hepatic FFA level. Such changes might be due to direct effects of IH on the intrinsic regulation of FFA uptake via CD36 expression by the liver. The findings of a reduction in hepatic CD36 expression, together with a lower hepatic FFA level in obesity, a main source of lipids in the liver, support the role of CD36 in the regulation of lipid profiles. In line with one previous study in ob/ob mice [46], CD36 deletion exacerbated hepatic steatosis by impairing hepatic triglyceride secretion via elevation of prostaglandin levels. However, the mechanisms and functional significance of a reduction in hepatic CD36 expression after IH in the diet-induced obese mice remain unclear. In mouse liver, CD36 is expressed on hepatocytes at low expression level but increases during hypoxia, possibly due to enhance hepatic uptake of FFA mobilized from adipose tissue via activation of the transcription factors like HIF-1α and HIF-2α [47–49]. HIF-1α mainly regulates glycolysis, while HIF-2α mainly regulates FAO [50]. In support, our data showed that IH induced HIF-1α activation, suggesting the promotion of glycolysis. However, further investigation is needed in order to explore HIF-2α stabilization and its impact on FAO during IH.

Despite unraveling novel evidence that IH featuring OSA led to liver injury via inflammatory infiltrates and collagen deposition with differential regulation of hepatic CD36 expression in lean and diet-induced obese mice, there are still limitations warranted for further investigations before a conclusive statement can be made. Firstly, it is uncertain whether the hypoxic episode (30 cycles per hour) that was adopted in our animal model is relevant to human OSA in the study of liver injury due to the limitation of IH-exposed animal model. The adopted hypoxic profile has been previously described using a pulse oximeter [19]. Secondly, the selected time point of 4-week IH exposure might only reflect the early changes of liver injury. Future studies should be extended to

add longer time points of IH exposure for further investigating the transitions from simple fatty liver into steatohepatitis and liver fibrosis in lean and diet-induced obese mice. Finally, this is a descriptive and observational study limiting the interpretation of a causal link between oxidative/inflammatory status, lipid profile, and hepatic histological assessment at this stage. The use of *Cd36*-knockout mice is needed to elucidate the complex interplay and to evaluate the mechanistic studies on the protective and detrimental pathways in the IH-exposed mouse model.

In conclusion, our data indicated that IH, a hallmark of OSA, causes differential regulation of hepatic CD36 expression in lean and diet-induced obese mice despite consistent features of liver injury with the increase in inflammatory cell infiltrates and collagen deposition in the liver, probably via oxidative and inflammatory mechanisms. Our findings shed light on IH-induced hepatosteatosis without or with obesity, which may be relevant to the understanding of the hypothesized role of OSA in the pathogenesis of NAFLD.

Author contributions

YJ, YL, MSMI and JCWM designed the study. YJ and YL performed the study, collected the data, carried out data analysis, and produced the initial draft of the manuscript. PHC, MG and SCY performed the study, collected the data and carried out data analysis. MSMI and JCWM contributed to revising the manuscript. All authors read and approved the final submitted manuscript.

Conflicts of interest

The authors have no Conflicts of interest to declare.

Acknowledgments

Appendix A. Supplementary data

Supplementary data to this article can be found online at https://doi.org/10.1016/j.bj.2022.10.003.

REFERENCES

[1] Fietze I, Laharnar N, Obst A, Ewert R, Felix SB, Garcia C, et al. Prevalence and association analysis of obstructive sleep apnea with gender and age differences - results of SHIP-Trend. J Sleep Res 2019;28(5):e12770.

[2] Abbasi A, Gupta SS, Sabharwal N, Meghrajani V, Sharma S, Kamholz S, et al. A comprehensive review of obstructive sleep apnea. Sleep Sci 2021;14(2):142−54.

[3] Gunduz C, Basoglu OK, Hedner J, Zou D, Bonsignore MR, Hein H, et al. Obstructive sleep apnoea independently predicts lipid levels: data from the European Sleep Apnea Database. Respirology 2018;23(12):1180−9.

[4] Mesarwi OA, Loomba R, Malhotra A. Obstructive sleep apnea, hypoxia, and nonalcoholic fatty liver disease. Am J Respir Crit Care Med 2019;199(7):830−41.

[5] Aron-Wisnewsky J, Clement K, Pépin JL. Nonalcoholic fatty liver disease and obstructive sleep apnea. Metabolism 2016;65(8):1124−35.

[6] Agrawal S, Duseja A, Aggarwal A, Das A, Mehta M, Dhiman RK, et al. Obstructive sleep apnea is an important predictor of hepatic fibrosis in patients with nonalcoholic fatty liver disease in a tertiary care center. Hepatol Int 2015;9(2):283−91.

[7] Powell EE, Wong VW, Rinella M. Non-alcoholic fatty liver disease. Lancet 2021;397(10290):2212−24.

[8] Mirrakhimov AE, Polotsky VY. Obstructive sleep apnea and non-alcoholic Fatty liver disease: is the liver another target? Front Neurol 2012;3:149.

[9] Polotsky VY, Patil SP, Savransky V, Laffan A, Fonti S, Frame LA, et al. Obstructive sleep apnea, insulin resistance, and steatohepatitis in severe obesity. Am J Respir Crit Care Med 2009;179(3):228−34.

[10] Aron-Wisnewsky J, Minville C, Tordjman J, Levy P, Bouillot JL, Basdevant A, et al. Chronic intermittent hypoxia is a major trigger for non-alcoholic fatty liver disease in morbid obese. J Hepatol 2012;56(1):225−33.

[11] Ng SSS, Wong VWS, Wong GLH, Chu WCW, Chan TO, To KW, et al. Continuous positive airway pressure does not improve nonalcoholic fatty liver disease in patients with obstructive sleep apnea. A randomized clinical trial. Am J Respir Crit Care Med 2021;203(4):493−501.

[12] Qi JC, Huang JC, Lin QC, Zhao JM, Lin X, Chen LD, et al. Relationship between obstructive sleep apnea and nonalcoholic fatty liver disease in nonobese adults. Sleep Breath 2016;20(2):529−35.

[13] Nguyen P, Leray V, Diez M, Serisier S, Le Bloc'h J, Siliart B, et al. Liver lipid metabolism. J Anim Physiol Anim Nutr 2008;92(3):272−83.

[14] Hajri T, Abumrad NA. Fatty acid transport across membranes: relevance to nutrition and metabolic pathology. Annu Rev Nutr 2002;22:383−415.

[15] Bonen A, Chabowski A, Luiken JJ, Glatz JF. Is membrane transport of FFA mediated by lipid, protein, or both? Mechanisms and regulation of protein-mediated cellular fatty acid uptake: molecular, biochemical, and physiological evidence. Physiology 2007;22:15−29.

[16] Koonen DP, Jacobs RL, Febbraio M, Young ME, Soltys CL, Ong H, et al. Increased hepatic CD36 expression contributes to dyslipidemia associated with diet-induced obesity. Diabetes 2007;56(12):2863−71.

[17] Buque X, Martinez MJ, Cano A, Miquilena-Colina ME, Garcia-Monzon C, Aspichueta P, et al. A subset of dysregulated metabolic and survival genes is associated with severity of hepatic steatosis in obese Zucker rats. J Lipid Res 2010;51(3):500−13.

[18] Rey E, Del Pozo-Maroto E, Maranon P, Beeler B, Garcia-Garcia Y, Landete P, et al. Intrahepatic expression of fatty acid translocase CD36 is increased in obstructive sleep apnea. Front Med 2020;7:450.

[19] Ge MQ, Yeung SC, Mak JCW, Ip MSM. Differential metabolic and inflammatory responses to intermittent hypoxia in substrains of lean and obese C57BL/6 mice. Life Sci 2019;238:116959.

[20] Zou W. Total lipid extraction. Protocol Exchange 2011.

[21] Liang W, Menke AL, Driessen A, Koek GH, Lindeman JH, Stoop R, et al. Establishment of a general NAFLD scoring system for rodent models and comparison to human liver pathology. PLoS One 2014;9(12):e115922.